Effect of size reduction on the ferromagnetism of the manganite $La_{1-x}Ca_xMnO_3$ (x=0.33)

2010 New J. Phys. 12 123026

(http://iopscience.iop.org/1367-2630/12/12/123026)

New Journal of Physics
The open-access journal for physics

Effect of size reduction on the ferromagnetism of the manganite $La_{1-x}Ca_xMnO_3$ ($x = 0.33$)

Tapati Sarkar[1,3,4], **A K Raychaudhuri**[1,3], **A K Bera**[2] and **S M Yusuf**[2]

[1] DST Unit for NanoSciences, S N Bose National Centre for Basic Sciences, Block JD, Sector III, Salt Lake, Kolkata 700 098, West Bengal, India
[2] Solid State Physics Division, Bhabha Atomic Research Centre, Mumbai 400 085, India
E-mail: tapatis@bose.res.in and arup@bose.res.in

New Journal of Physics **12** (2010) 123026 (21pp)
Received 4 August 2010
Published 16 December 2010
Online at http://www.njp.org/
doi:10.1088/1367-2630/12/12/123026

Abstract. In this paper, we report an investigation of the ferromagnetic state and the nature of ferromagnetic transition of nanoparticles of $La_{0.67}Ca_{0.33}MnO_3$ using magnetic measurements and neutron diffraction. The investigation was performed on nanoparticles with crystal size down to 15 nm. The neutron data show that even down to a size of 15 nm the nanoparticles show finite spontaneous magnetization (M_S) although the value is much reduced compared to the bulk sample. We observed a non-monotonic variation of the ferromagnetic-to-paramagnetic transition temperature T_C with size d and found that T_C initially enhances upon size reduction, but for $d < 50$ nm it decreases again. The initial enhancement in T_C was related to an increase in the bandwidth that occurred due to a compaction of the Mn–O bond length and a straightening of the Mn–O–Mn bond angle, as determined from the neutron data. The size reduction also changes the nature of the ferromagnetic-to-paramagnetic transition from first order to second order with critical exponents approaching mean field values. This was explained as arising from a truncation of the coherence length by the finite sample size.

[3] Authors to whom any correspondence should be addressed.
[4] Present address: Laboratoire CRISMAT, UMR 6508 CNRS ENSICAEN, 6 bd Maréchal Juin, 14050 CAEN, France. E-mail: tapati.sarkar@ensicaen.fr

Contents

1. Introduction

The effect of size reduction on physical properties of hole-doped manganites is a topic of considerable interest. The properties of nanoparticles of manganites (often called 'nanomanganites') have been investigated recently [1]–[10]. In general, the properties of nanoparticles of magnetic materials can arise from intrinsic properties, or from factors arising from interactions of nanoparticles [11, 12]. In this paper, we address issues that arise from intrinsic factors in the specific context of nanoparticles of perovskite oxide $La_{0.67}Ca_{0.33}MnO_3$. In manganites, the existence of competing interactions that arise from orbital, charge and spin degrees of freedom makes them an interesting system. The manganites exhibit a wide spectrum of physical properties leading to rich phase diagrams arising from these competing interactions [13]. Thus, the investigation of the effect of size reduction on such a system with a multitude of competing interactions makes for a very interesting study. In particular, it is important to understand how the finite size affects various aspects of the ferromagnetic state including the nature of the paramagnetic to ferromagnetic transition.

The physical properties of manganites arise from two generic broad classes of competing effects, namely the charge and orbital order that lead to insulating and generally antiferromagnetically (AFM) ordered ground state, and the double-exchange interactions that lead to metallic and ferromagnetically (FM) ordered ground state. These interactions can be tuned by a number of external parameters and also internal parameters such as the carrier concentration, structure and ionic size. The resulting ground state thus depends on the relative strength of these two competing interactions. In the nanomanganites, an additional factor, namely the size, becomes important and can tune these competing interactions and even change the nature of the ground state. In this paper, we investigate the effects of size reduction on ferromagnetic nanoparticles of $La_{0.67}Ca_{0.33}MnO_3$ down to a size of 15 nm by using magnetic measurements as well as neutron diffraction that gives information both on the magnetic state and on the structure. We note that while bulk magnetic measurements have been used in the past to study nanoparticles of manganites, neutron diffraction studies have not been used to study

the structure and magnetism of these ferromagnetic nanoparticles. In this work, we specifically address the following issues: (a) the change in the ferromagnetic transition temperatures on size reduction, (b) the reduction in the spontaneous magnetic moment and (c) the important issue of change in the nature of the ferromagnetic to paramagnetic transition from first order to second order on size reduction.

Out of all the doped manganites, nanoparticles of $La_{0.67}Ca_{0.33}MnO_3$ (LCMO) are perhaps the most widely studied system [1, 10, 14, 15]. The ferromagnetic films of $La_{0.67}Ca_{0.33}MnO_3$ with thickness down to a few tens of nm have also been investigated to look for the effects of size reduction on the ferromagnetic-to-paramagnetic transition temperature T_C [16]. However, quite contradictory results have been published by different groups as to what happens to the ferromagnetic T_C as the particle size (diameter d) is reduced [1, 14, 15]. The results range from enhancement of T_C, reduction of T_C as well as no change in T_C as d is reduced. We re-examine this apparently conflicting issue by making particles of sizes over a large range (down to 15 nm), which has not been done before, using the same synthesis method. We establish the crucial observation that size reduction leads to a shallow but distinct strengthening of T_C down to a size of nearly 50–75 nm and then, on further size reduction, we find that the T_C is suppressed as the size is taken down to 15 nm. Interestingly, in this size range the spontaneous magnetization M_S, as measured by the neutron diffraction data, shows that although a magnetic order still exists in the bulk of the nanocrystals even down to 15 nm, there is a substantial reduction in the average value of M_S. By comparing our data on $La_{0.67}Ca_{0.33}MnO_3$ with those obtained in nanoparticles of $La_{0.5}Sr_{0.5}CoO_3$, which is not a double-exchange ferromagnet, we establish that the enhancement of T_C seen in the initial stage of size reduction ($d > 50$ nm) is a special feature of the manganites.

Our earlier work on half-doped manganite nanocrystals [17, 18] has shown that the charge and orbitally ordered ground state is affected by the structural changes occurring in the system on size reduction. This led us to believe that a study of how the structure of the $La_{0.67}Ca_{0.33}MnO_3$ nanocrystals evolves on size reduction might well shed some light on its magnetic properties. This paper thus investigates whether size reduction in $La_{0.67}Ca_{0.33}MnO_3$ leads to any change in the crystal structure symmetry, or whether there are any changes in the values of the structural parameters. Such a detailed structural study of nanocrystals of LCMO has not been performed before.

The issue of the order of paramagnetic-to-ferromagnetic phase transition in manganites is a topic of considerable interest. Manganite with composition $La_{0.67}Ca_{0.33}MnO_3$ shows a first-order phase transition at the paramagnetic-to-ferromagnetic transition [19]–[22] in the bulk form. This is a special feature of the hole-doped system $La_{1-x}Ca_xMnO_3$. This happens for $x \approx 0.2$–0.4. For $x \leqslant 0.2$, the transition is second order with critical exponents close to what one would expect for a three-dimensional (3D) Heisenberg system. For $x \geqslant 0.4$, the first-order transition ends in continuous transition at a tricritical point [23]. For other manganites with Sr or Ba substitution instead of Ca [24], the paramagnetic-to-ferromagnetic transition is second order. It thus appears that, depending on the bandwidth and/or carrier concentration, the nature of the transition can change. We have investigated the effect of size reduction on the nature of the phase transition in the $La_{0.67}Ca_{0.33}MnO_3$ system and found that the first-order transition changes over to a continuous (second order) transition on reducing the size, and the exponents approach a value close to that predicted by the mean-field theory. We believe that this particular aspect has not been investigated before in nanoparticles of manganites.

Table 1. Sample ID, average particle diameter (d), oxygen deficiency (ϵ), ferromagnetic Curie temperature (T_C) and coercive field (H_C) of LCMO samples used for neutron diffraction studies.

Sample ID	d (nm)	ϵ	T_C from M–T measurements (K)	T_C from neutron data (K)	H_C (mT) at $T = 80$ K
A	15 ± 2	0.02	242	234	20
B	50 ± 15	0.04	294	291	23
C	300 ± 40	0.03	277	274	10
D	21500 ± 2000	0.05	265	268	3

2. Experimental

The samples were prepared by a standardized chemical synthesis route and were well characterized using techniques such as x-ray diffraction (XRD)[5] and imaging tools such as transmission electron microscopy (TEM)[6] and scanning electron microscopy (SEM)[7]. The details of the synthesis method can be found in one of our earlier publications [17]. We could grow a batch of samples with varying particle diameter (see table 1) using the same synthesis technique. The chemical (cation) stoichiometry was checked using the inductively coupled plasma atomic emission spectroscopy (ICPAES) technique, and the oxygen stoichiometry was checked using iodometric titration. All our samples had slight oxygen deficiency ($La_{0.67}Ca_{0.33}MnO_{3-\epsilon}$) with ϵ positive. $\epsilon \approx 0.02$ for the sample with the smallest particle diameter and it increased somewhat for the bulk sample. Thus, the particles with smaller particle diameter have somewhat better oxygen stoichiometry. A list of the samples used for the neutron diffraction studies is shown in table 1.

The Curie temperatures quoted in table 1 have been established from magnetization measurements as well as from the neutron data. All the magnetic measurements were carried out using a vibrating sample magnetometer[8]. The average particle diameter was estimated from XRD results (using the Williamson Hall plot [25]) as well as from imaging tools such as TEM for smaller particles and SEM for larger particles. The latter also gave us the size distribution in each sample. The single crystallinity of the particles was also checked using TEM. Figure 1 gives the representative TEM and SEM data for particles with extreme sizes (samples A and D in table 1). Based on the extensive TEM data, we find that the nanoparticles of size range below 100 nm are single nanocrystals. We will thus use the terms 'nanoparticles' and 'nanocrystals' interchangeably.

The neutron diffraction experiments on these samples were carried out at the Dhruva reactor (beam port T1013) in Bhabha Atomic Research Centre, Mumbai, India. The wavelength used was 1.249 Å and the scattering angular range covered was $2\theta = 5^\circ$–140° with a step size of 0.05°. The powders were packed in a vanadium can of height 35 mm and diameter 6 mm. For low temperature scans, a closed cycle refrigerator was used. This diffractometer has a flux of 8.5×10^5 neutrons $cm^{-2}\,s^{-1}$ and a beam size of 4 cm × 1.5 cm. There is a total of five linear

[5] X'Pert PRO Diffractometer, PANanalytical BV, Lelyweg 1, 7602 EA Almelo, The Netherlands.
[6] JEOL 200 kV, JEOL Ltd, 1–2, Musashino 3—chome Akishima, Tokyo 196-8558, Japan.
[7] FEI Quanta 200, FEI Company, North America NanoPort, 5350, NE Dawson Creek Drive, Hillsboro, OR 97124, USA.
[8] Lake Shore Cryotronics, Inc. 575 Mc Corkle Blvd, Westerville, OH 43082, USA.

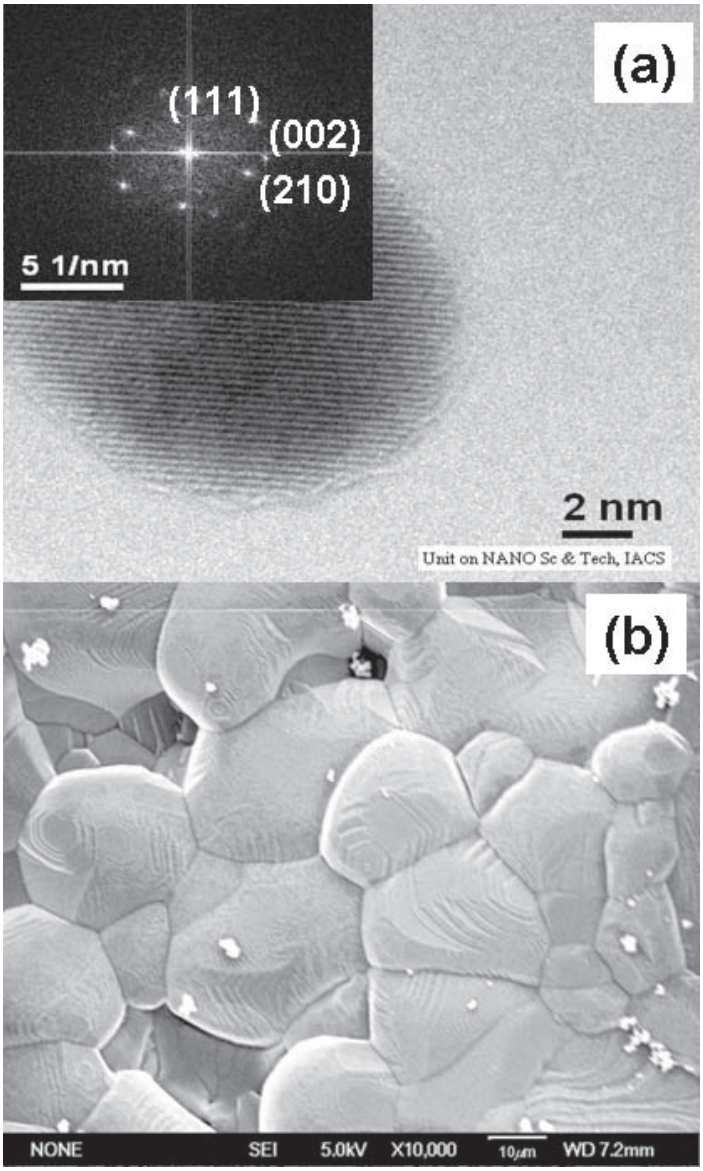

Figure 1. (a) TEM image of LCMO-A showing a single nanoparticle of size ∼15 nm and (b) SEM image of LCMO-D. The inset in (a) shows the electron diffraction pattern taken on LCMO-A.

position sensitive detectors that allows the Q range to vary from 0.4 to 9.4 Å^{-1}. The Rietveld analyis of the structure (both lattice and magnetic structure) was done using FullProf Suite software [26].

3. Results

3.1. Ferromagnetic T_C and its dependence on size

The Curie temperatures of the samples were determined from the magnetization data measured at a field of $H = 1$ mT. The representative data on field-cooled (FC) and zero field-cooled (ZFC) magnetization (M) versus temperature (T) curves for the samples are shown in figure 2.

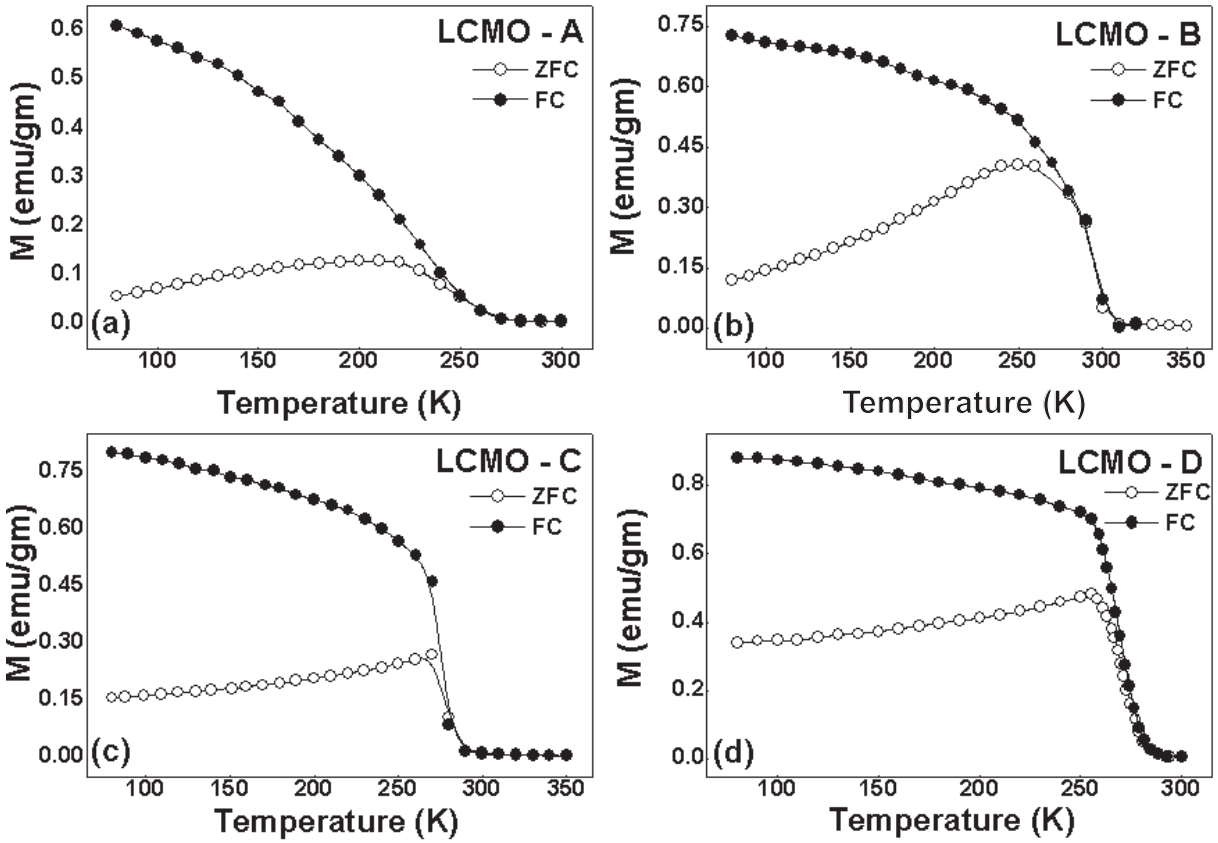

Figure 2. ZFC and FC M versus T curves for LCMO samples with different average particle diameters.

The samples show a ferromagnetic transition temperature T_C down to the lowest sample size (LCMO-A). Although not shown here, we have obtained well-defined hysteresis loops for all the samples, including the sample with the smallest size. At $T = 80$ K, the coercive field H_C changes from a rather low value of 2 mT for the bulk sample to about 20 mT for sample A as shown in table 1. The temperature and size variation of H_C in these materials are interesting but a detailed study of this issue is not within the scope of the paper. The magnetic data show that the samples that we are working with remain ferromagnetic even after size reduction of more than three orders of magnitude, although there is a distinct variation of T_C as well as the absolute value of the magnetization with size as described below.

In figure 3, we show the variation of T_C with particle diameter (d). The graph also has data on samples of additional sizes on which magnetization data were taken but neutron data were not taken and they are not shown in table 1. The T_C was identified from the inflection points in the dM/dT versus T plots. In the same figure, we also plot the T_C values as obtained from the neutron diffraction data (we elaborate on the neutron diffraction measurements in the next section). The data obtained from the two methods are very close except for the smallest sample, where the neutron data show somewhat less ($\approx$3%) T_C. This is understandable because the magnetic transition in the smaller size nanoparticles is broader, which does introduce some uncertainty in its determination. Also, in the neutron data a clear T_C can be seen only when a long-range magnetic correlation builds up so that the intensity that adds on to a structural

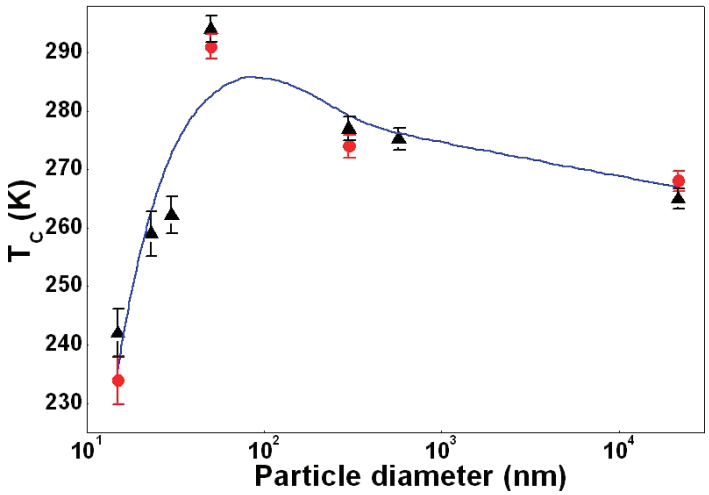

Figure 3. Variation of T_C with d in $La_{0.67}Ca_{0.33}MnO_3$ nanoparticles. T_C obtained from the magnetization data (black triangles) as well as from the neutron data (red circles) are shown. The line is a fit to the data using equation (5) (see the discussion section).

peak can be clearly distinguished. The identification of a clear T_C by the neutron data is thus significant because it denotes the onset of bulk ferromagnetic order in an appreciable part of the sample. We also note that no previous studies have settled this issue of whether long-range ferromagnetic order indeed exists in such small manganite nanoparticles of size as small as 15 nm. We discuss this issue again later on.

We note here that by varying the particle size over such a wide range, we find that our samples show a non-monotonic variation of the Curie temperature with d. This is unlike earlier reports on magnetic studies of LCMO nanocrystals (done with a limited range of particle size), which reported a monotonic variation or no variation of T_C with particle diameter [1, 14]. This result, i.e. a non-monotonic variation of T_C with size, is thus new. We will show below that it points to interesting physics where we have a likely combination of finite size effects and effects due to variation of the bandwidth working in tandem. The size where the turnaround in T_C occurs is for $d \approx 50$ nm, and we will show that there is a reduction of the magnetic moment (as determined from the neutron data) in this size range.

We observe that the region of turnaround in T_C is somewhat sensitive to the method of sample preparation/heat treatment temperatures, and variations in T_C of $\approx \pm 5\%$ can be seen in the size range $d \approx 70$–100 nm (where the turnaround occurs) depending on the sample preparation conditions. The sample preparation conditions change the size distribution even if the average size is the same. Since T_C has a non-monotonic dependence on d, this makes the average value of the observed T_C rather sensitive to the exact size distribution, leading to variations in T_C for the same average size d.

3.2. Lattice and magnetic structures from neutron data

An important issue that the paper probes is whether there is indeed a change in the lattice as well as the magnetic structure (including the spontaneous magnetization) on size reduction and whether the observed changes in magnetic properties can have a structural basis. This

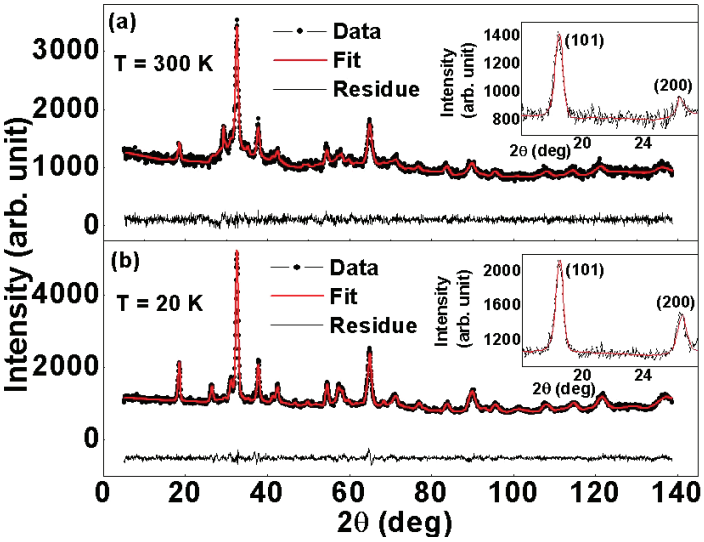

Figure 4. Neutron diffraction patterns for the nanoparticles with size 15 nm (LCMO-A) taken at (a) $T = 300$ K and (b) $T = 20$ K. The insets show the expanded regions between $2\theta = 16^\circ$ and 27.5°. The lines through the data points are the results of profile fitting. The residues are shown at the bottom.

is relevant in the light of our earlier studies [17, 18], which have shown that the crystal structure is strongly related to the orbitally ordered ground state of these systems in the regime of carrier concentration where there is charge ordering. For this purpose, neutron diffraction measurements were carried out on four representative samples (listed in table 1). This gave us a dual advantage of being able to probe the lattice as well as the magnetic structure. The data were taken at different temperatures from 20 to 320 K. A detailed two-phase Rietveld refinement (with a structural phase and a magnetic phase) was done to extract the various structural and magnetic parameters. The space group *Pnma* was used for both phases. The line profiles were modeled using a pseudo-Voigt profile shape function. As an example, in figure 4, we show the neutron diffraction patterns for LCMO-A (along with the fits) taken at (a) $T = 300$ K and (b) $T = 20$ K. In the corresponding insets, we have shown the expanded regions between $2\theta = 16^\circ$ and 27.5° to show the two Bragg peaks ((101) and (200)), where the magnetic contribution has been observed. $La_{0.67}Ca_{0.33}MnO_3$ being ferromagnetic, the magnetic contribution occurs at the same 2θ values as the structural peaks. The enhancement of the Bragg peak intensity with decreasing temperature (as can be seen clearly from a comparison of the intensities in the insets of figure 4) confirms the presence of ferromagnetic ordering in the sample with the lowest particle size.

The Rietveld refinement was used to obtain the lattice parameters as well as the bond angles and bond lengths of the samples. The temperature evolution of the lattice parameters shows that there are no large lattice distortions at the transitions but the lattice shows a small contraction at the magnetic transition. This is similar to that found in manganites such as $La_{0.7}Sr_{0.3}MnO_3$ [27]. The coefficient of thermal expansion (α) calculated from the temperature dependence of the cell volume shows that the value of α remains almost unchanged at $\approx 1 \times 10^{-5}\,K^{-1}$ despite a decrease in particle diameter by three orders. The evolution of the lattice parameters and cell volume with size at two temperatures ($T = 20$ and 300 K) is shown in figure 5. There

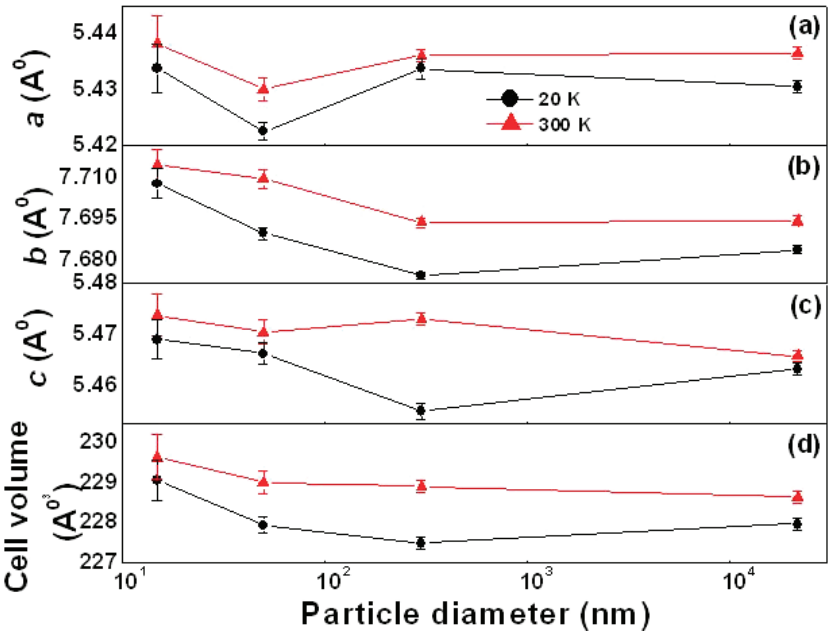

Figure 5. Variation of (a) a, (b) b, (c) c and (d) unit cell volume with particle diameter at $T = 20$ and 300 K for LCMO.

is not much change in the cell volume except for the smallest size sample where it shows a small increase. This is in sharp contrast to the half-doped $La_{0.5}Ca_{0.5}MnO_3$ [17, 18] where size reduction leads to a distinct contraction in the cell volume.

The analysis of the neutron data shows that a clear change, although small, occurs in the MnO_6 octahedron on size reduction as revealed through the Mn–O–Mn bond angles and Mn–O bond lengths. These two parameters have a direct role in the determination of the overlap integral and thus of the bandwidth W. In figure 6, we show the temperature dependence of the two Mn–O–Mn bond angles for the samples studied. Bond angles Mn–O_1–Mn and Mn–O_2–Mn refer to the apical (O_1) and equatorial (O_2) oxygen atoms. In figure 7, the temperature variations of the two bond lengths for the samples are shown. The size reduction thus leads to a gradual compaction of the Mn–O bond lengths and Mn–O–Mn bond angles move closer to 180° for the apical oxygen. Both of these are expected to enhance the bandwidth W.

The unit cell of the manganites is often distorted from the cubic structure. The Jahn–Teller distortion around the Mn^{3+} ions leads to orthorhombic distortions. The reduction of the orthorhombic distortion strengthens the double-exchange interaction, enhances the bandwidth and strengthens the ferromagnetic state. Ferromagnetic composition $La_{0.67}Ca_{0.33}MnO_3$ has low orthorhombic strains. The orthorhombic distortion can be quantified by orthorhombic strains ($O_{S_\parallel}$ and $O_{S_\perp}$), which give a measure of the deviation of the unit cell from the perfect cubic structure. We define the orthorhombic strains as $O_{S_\parallel} = 2(c-a)/(c+a)$ (giving the strain in the ac plane), and $O_{S_\perp} = 2(a+c-b\sqrt{2})/(a+c+b\sqrt{2})$ (giving the strain along the b-axis with respect to the ac plane). In figure 8, we show the evolution of the orthorhombic strains as a function of temperature for the four samples. We find that there is a small but very discernible reduction in the $O_{S_\perp}$ strains on size reduction. (Note: the strains are small and have been calculated by taking the differences of two relatively large but nearly equal

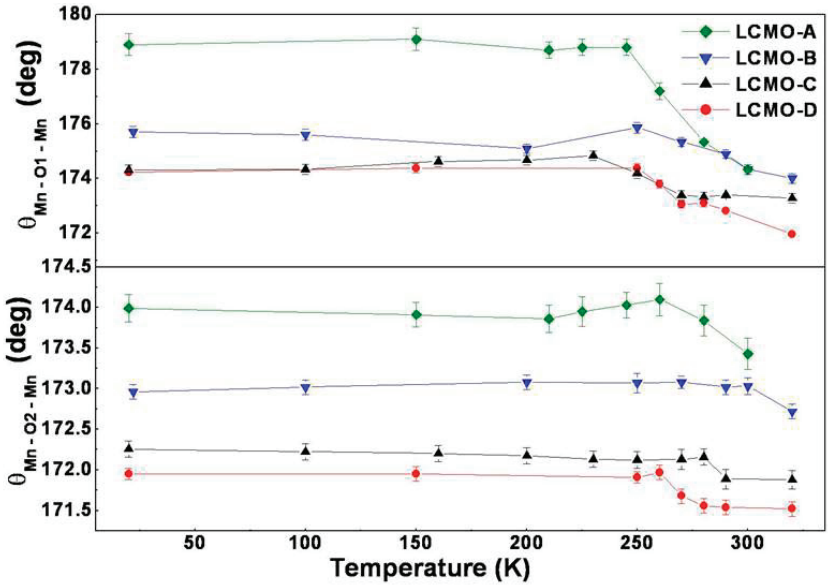

Figure 6. Variation of the Mn–O–Mn bond angle with temperature for LCMO with varying particle diameters.

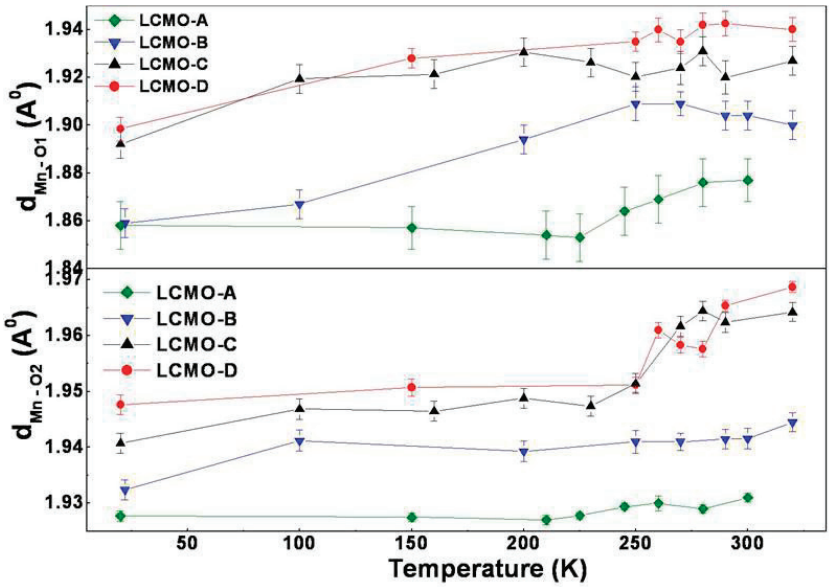

Figure 7. Variation of the Mn–O bond length with temperature for LCMO with different particle diameters.

quantities. This enhances the error bar on the strain data.) At this stage, it will be worthwhile to compare the structural changes with compositions that are more distorted. In half-doped $La_{0.5}Ca_{0.5}MnO_3$, due to Jahn–Teller distortion, the onset of charge and orbital ordering leads to strong orthorhombic strain, which gets qualitatively affected upon size reduction. In the ferromagnetic $La_{0.67}Ca_{0.33}MnO_3$, the orthorhombic strain is low to start with and thus there is no large effect on this strain upon size reduction. Thus, there is a fundamental difference in the structure of nanocrystals of these compositions that show different ground states.

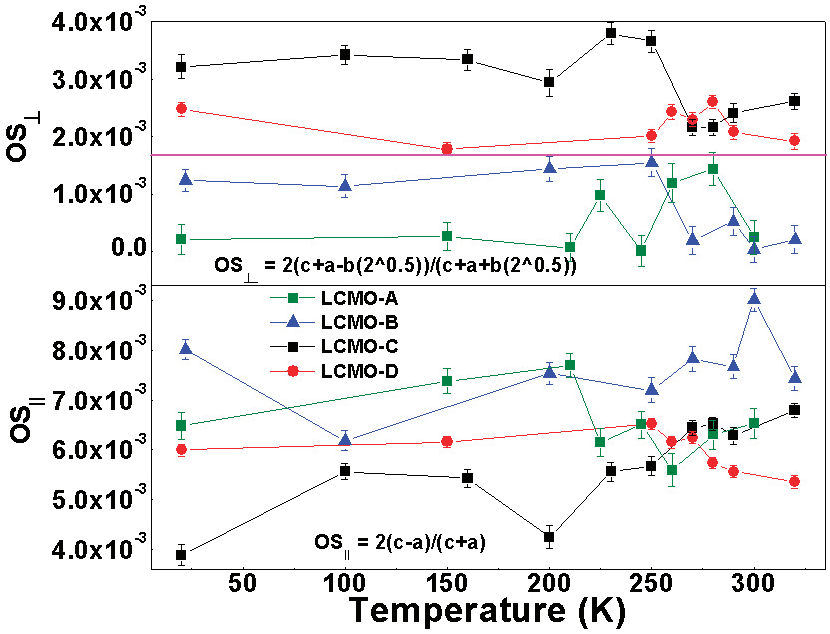

Figure 8. Variation of $O_{S_\parallel}$ (lower panel) and $O_{S_\perp}$ (upper panel) with temperature for $La_{0.67}Ca_{0.33}MnO_3$ with varying particle diameters. The pink line in the upper panel shows a demarcation between the larger and smaller diameter particles.

The analysis of structural data as obtained from the neutron data clearly shows that the size reduction even down to a diameter of 15 nm retains the basic perovskite structure and does not distort it in any significant way. The small yet clear change that occurs is that the MnO_6 octahedra become somewhat more compact and the Mn–O–Mn angle, both for the apical and equatorial oxygen, moves closer to 180°. Such a change, as we will see below, can lead to an enhancement of the bandwidth.

3.3. Variation of spontaneous magnetization M_S with T and d

Neutron data allow us to obtain the spontaneous magnetization (M_S), which is measured at zero applied field. This allows us to answer a fundamental question whether the manganite nanoparticles have a spontaneous magnetization that arises from long-range ferromagnetic order. In figure 9, we show the variation of M_S as a function of T for the samples studied. The variation of M_S at $T = 20$ K as a function of the diameter d is shown in figure 10. The value of M_S remains close to the bulk value down to $d = 50$ nm and then shows a downturn as the size is reduced further. One may note from figure 3 that the T_C shows an increase till the size is reduced to this value ($d = 50$ nm) and then shows a sharp drop when the size is reduced further. It is to be noted, however, that even in the smallest sample ($d = 15$ nm), there is ferromagnetic order and a finite spontaneous magnetization M_S although it is reduced considerably from the bulk value.

3.4. Nature of the magnetic phase transition in manganite nanocrystals

As a part of the investigation of ferromagnetic nanocrystals of $La_{0.67}Ca_{0.33}MnO_3$, we have investigated what happens to the first-order ferromagnetic-to-paramagnetic phase transition

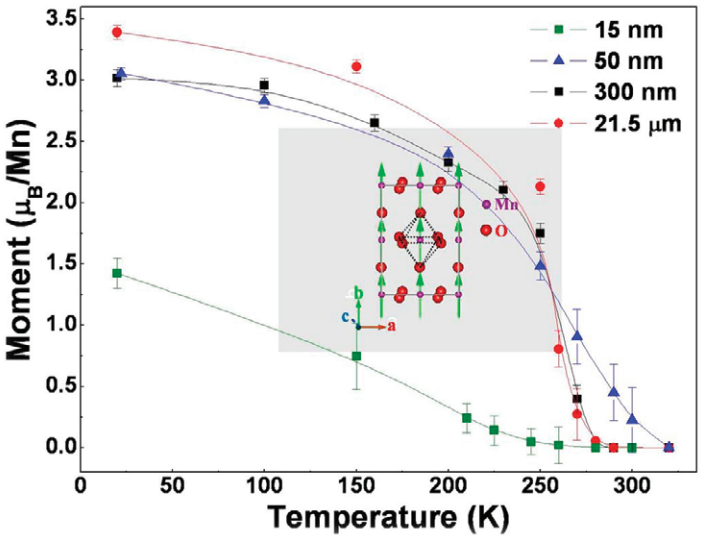

Figure 9. Variation of the spontaneous moment with temperature for LCMO-A, LCMO-B, LCMO-C and LCMO-D. The inset shows a schematic representation of the magnetic structure with all the moments aligned along the *b*-axis.

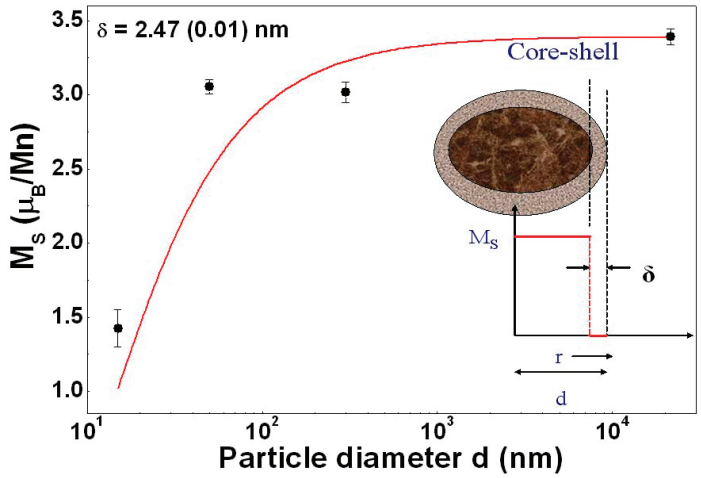

Figure 10. Variation of spontaneous moment at $T = 20\,\mathrm{K}$ as a function of the average particle diameter (d). The red line is obtained from the core–shell model using equation (1) (see the discussion section). The inset shows a schematic representation of the core–shell model for the nanoparticles.

upon size reduction. The nature of the magnetic transition can be obtained from the slope of isotherm plots of M^2 versus H/M, M being the experimentally observed magnetization and H the magnetic field. This criterion for deciding the nature of the transition is generally referred to as the Banerjee criterion [28] and has been widely used to experimentally determine the order of the magnetic phase transition. Briefly, a positive or a negative slope of the experimental H/M versus M^2 curve indicates a second-order or a first-order transition, respectively. In the context of materials undergoing second-order transition, such a plot is called an Arrott plot. For

materials showing first-order magnetic transition, an Arrott plot of the type seen for a second-order transition will not occur. We have applied this criterion to the LCMO samples with two widely different particle diameters but with a T_C that is rather close. Interestingly, we found striking differences in the magnetic behavior of the two samples around T_C. This crossover of the first-order transition to the second-order transition on size reduction has not been reported before for manganites. There are, however, reports of a change in the nature of transition from first order to second order in the AFM transition in MnO nanoparticles supported in a porous matrix with sizes down to 14 nm [29].

Here we note that the presence or absence of hysteresis in M versus T can also be used to establish the nature of the phase transition (presence of hysteresis in field-cooled cooling (FCC) and field-cooled warming (FCW) data in the case of first-order phase transition and absence of the same in the case of second-order phase transition). However, in the specific case of bulk $La_{0.67}Ca_{0.33}MnO_3$, the phase transition appears to be weakly first order. The thermal hysteresis observed in FCC and FCW data is very small (<2 K) [30]. As a result, using the hysteresis criteria appears to be difficult. The Banerjee criterion provides a more striking and straightforward way to distinguish between samples showing a first-order transition and those showing a second-order transition, because the slope of the M^2 versus H/M curves changes sign. In addition, exploring the nature of the phase transition through the Banerjee criterion offers us the advantage of determining the critical exponents for the sample exhibiting a second-order phase transition.

The choice of the samples was guided by the variation of T_C with d as shown in figure 3. It can be seen that samples with $d \approx 30$ nm are expected to have T_C close to the bulk value. The investigation was thus carried out on a sample with average $d \approx 23$ nm (referred to as SAMPLE-E) that has $T_C \approx 260$ K, which is close to the $T_C = 265$ K of the 'bulk sample' (SAMPLE-D) that has an average size of $d = 21.5\ \mu$m, which is three orders larger.

We have measured the initial magnetization isotherms in the close vicinity (± 10 K) of T_C. The critical exponents for the continuous transition have been measured for $\epsilon = |T - T_C|/T_C < 4 \times 10^{-2}$. Before each run, samples were heated above their T_C and cooled to the measuring temperature under zero field in order to ensure perfect demagnetization of the samples. In figure 11, we plot M^2 versus H/M isotherms between 260 and 280 K for the bulk sample (SAMPLE-D). The deviation from the normal behavior expected from a second-order transition is very clear and this deviation is a signature of the first-order transition. It is clear that the isotherms present negative slopes in some parts that according to the criterion used here, is an indication of the first-order character of the transition. The observation of a first-order transition in the bulk sample is in agreement with previous studies [19, 20, 22].

The magnetization isotherms for the SAMPLE-E plotted as Arrott plots are shown in figure 12. The isotherms were recorded for the temperature range 250–270 K. It is seen that the isotherms do not display the anomalous change of slope as seen in the bulk sample. Here, we find a positive slope throughout the range of M^2. Nanoparticles of LCMO thus show a second-order magnetic phase transition at T_C. The exact values of the critical exponents β and γ and the exact Curie temperature T_C were determined from a modified Arrott plot by taking β, γ and T_C as parameters to be obtained from the fit. (The plot has not been shown to avoid duplication.) The exact values of the exponents are $\beta = 0.47 \pm 0.01$ and $\gamma = 1.06 \pm 0.03$. One can also obtain δ directly from the plot of M versus H at T_C. From such a plot, we obtain $\delta = 3.10 \pm 0.13$. The mean field value of the exponent δ can also be derived using $\delta = 1 + \frac{\gamma}{\beta}$. We find that $\delta = 3.26 \pm 0.16$. A comparison of the critical exponents shows that the magnetic

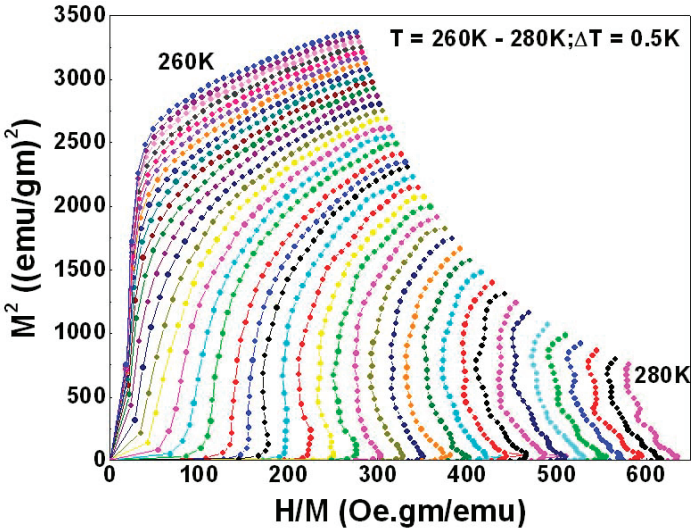

Figure 11. M^2 versus H/M plots for bulk LCMO (SAMPLE-D) with $d = 21.5\,\mu$m.

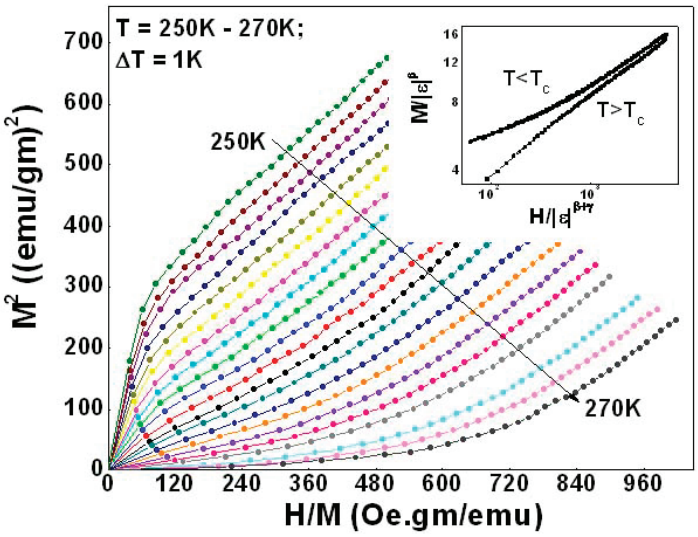

Figure 12. Arrott plots for nanocrystals of LCMO (SAMPLE-E) with $d = 23$ nm. The inset shows the scaling plots.

transition is not only second order but the exponents are closer to the mean field values $\beta = 0.5$, $\gamma = 1$ and $\delta = 3$ than what one would expect them to be for a 3D Heisenberg system ($\beta = 0.365$, $\gamma = 1.386$ and $\delta = 4.80$).

The critical exponents of the transition can be equivalently determined from scaling plots of the form $M/|\epsilon|^{\beta} = f_{\pm}(H/|\epsilon|^{\gamma+\beta})$, where $\epsilon = |T - T_C|/T_C$, $f_{\pm}$ is a scaling function and the plus and minus signs correspond to the ferromagnetic and paramagnetic regions, respectively. By appropriate selection of the parameters T_C, β and γ, the data should collapse on two different branches for $T > T_C$ and $T < T_C$. We construct scaling plots (shown in the inset of figure 12) to prove the validity of our choice of β, γ and T_C. A convincing scaling of the data points on the two branches of the scaling function $f_{\pm}$ can be seen.

We have thus observed a very clear change in the nature of the paramagnetic-to-ferromagnetic transition in LCMO from first order to second order when the particle diameter is brought down from bulk to a few tens of nanometers range. We note that the change in the nature of the phase transition by changing the size has not been reported before. Although we have not investigated the change in the nature of the transition by varying the particle sizes in close steps, the preliminary data that are available show that the crossover may occur for average sizes less than 200 nm.

4. Discussions

The results presented above show that there are important and subtle changes that occur in the magnetic properties upon size reduction in manganites. While the ferromagnetic state is retained down to a size of $d = 15$ nm, the magnetization is suppressed beyond a size of $d \approx 50$ nm. The observation that ferromagnetic T_C shows a non-monotonic dependence on the size is also interesting. While the suppression of T_C on size reduction may be expected due to such phenomena as the finite-size effect [16], the initial enhancement of T_C when the size is reduced to $\approx$50 nm is unusual. The size reduction also changes the nature of the ferromagnetic transition from first order to second order with critical exponents that are close to the mean field values. The crystal structure as obtained from the neutron data shows that there are small yet definite changes upon size reduction. These changes are much smaller than the qualitative changes seen in the half-doped composition that has strong orthorhombic strain. The basic perovskite structure of the bulk manganite is preserved although there is a clear compaction of the MnO_6 octahedra and the orthorhombic distortion $O_{S_\perp}$ is somewhat reduced. We will discuss below whether these small but definite changes upon size reduction have any effect on the magnetic properties. In the following subsections, we discuss the physical implications of the main observations.

4.1. Dependence of spontaneous magnetization M_S on size (d)

The size dependence of M_S has been shown in figure 10. Reduction of the saturation magnetization with size reduction has been seen in different types of magnetic nanoparticles previously [12], including manganite nanoparticles [10]. Our observation, however, is made on spontaneous magnetization (obtained with no applied field) as obtained from the neutron data. To explain the reduction of M_S with d, we propose a simple core–shell model. This is similar to that proposed for explaining reduction in saturation magnetization in magnetic nanoparticles in general [31]. The magnetic particles have ordered cores that can show long-range ferromagnetic order. We propose that the disordered shell (of thickness δ) does not have any spontaneous magnetization and is like a magnetic dead layer. There are recent TEM studies [9] that show that the surface of manganite nanowires has a layer of thickness $\approx$2 nm that is disordered. A close inspection of the TEM data of the type shown in figure 1 shows that in most of our nanoparticles there are layers of size $\sim$ 1–2 nm where no clear lattice fringes are seen. This would thus indicate the existence of structurally disordered regions at the surface. It may happen that the dead layer has spins that are aligned in random directions due to randomness of the local anisotropy field. These regions, however, lack any long-range order and it is expected that the spontaneous magnetization $M_S \to 0$ in this region. A schematic diagram of the core–shell model is shown in the inset of figure 10. If the shell thickness δ is indeed small, larger particles with

$d \gg \delta$ will not be affected, while for smaller particles, δ, although small, can be comparable to d and the measured magnetization, will thus be affected. The measured M_S is proportional to the volume fraction of the core that carries the spontaneous magnetization, i.e. $M_S = M_{0S}(\frac{d/2-\delta}{d/2})^3$, where M_{0S} is the spontaneous magnetization for a bulk sample that has long-range magnetic order. Expanding the cube and ignoring higher powers of (δ/d), we obtain

$$M_S = M_{0S}\left(1 - \frac{6\delta}{d}\right). \tag{1}$$

Equation (1) can be used to find the thickness δ of the shell. Generally, it is expected that δ may vary for particles of different sizes. However, we find that δ is rather similar for all sizes and we can fit the data to equation (1) with a more or less constant value of the shell thickness of $\delta \approx 2.47$ nm as shown by the red line in figure 10. The increasing importance of the disordered shell for the smaller diameter particles becomes apparent when we compare δ to the diameter of the particles (d). The rapid reduction of the M_S for small d can thus be understood. From the value of δ it can be seen that for nanocrystals with $d < 10$ nm the $M_S \to 0$ and it is likely that there will be no spontaneous moment for particles with $d \approx 5$ nm or less.

The thickness of the surface layer δ, estimated by the size dependence of the magnetization, is similar to that observed from direct TEM imaging [9]. This is also in agreement with estimation from local conductance mapping in nanostructured films of manganites as done by an STM [32]. In this context, we note that the estimation of the value of δ from spontaneous magnetization M_S as measured from neutron data can be different from that estimated from the magnetization data that is done with an applied field. This is because equation (1) assumes that $M_S = 0$ for the shell layer at the surface. However, the surface layer may lack long-range order, which may arise due to freezing of spins in random directions. In this case also M_S will be zero but it may show a finite value of magnetization when a field is applied to measure the magnetization. We note that there is indeed a controversy about the magnetic nature of the surface layer, which in some materials can show a low-temperature spin freezing that can be interpreted as a spin glass-like transition [7]. In the absence of a detailed study of the surface spin we cannot comment on the exact spin structure at the surface. However, whatever the nature of the disordered spins at the surface, it will lack long-range order and will have a zero value for the spontaneous magnetization. Thus, estimating the thickness of the 'dead' surface layer from the spontaneous magnetization M_S does not suffer from the ambiguity that may occur in estimates based on saturation magnetization data. (Note: the existence of disorder in the surface spins is often obtained from the high field susceptibility. Measurements of high field susceptibility in fields up to 1.5 T, which is much larger than the field for technical saturation, showed that there is no large change in the high field susceptibility upon size reduction.)

Here, we would like to note that the size of the smallest nanoparticles that we are working with ($\sim$15 nm) is of the same order as the particle size where the system may start to show superparamagnetic behavior. (A simple estimate based on the relative strengths of the exchange constant, J, and the bulk value of the saturation magnetization, M_S, for manganites yields the size of a single domain to be $\sim$25–30 nm.) However, in this paper, the specific issue of superparamagnetic behavior has not been investigated.

4.2. Dependence of transition temperature T_C on size d

In figure 3, we have shown the non-monotonic variation of T_C with d. In the initial stages of size reduction as we reduce the crystal size from the bulk, there is a clear enhancement of T_C.

However, beyond a certain size ($d < 50$ nm) the T_C rapidly decreases as d is reduced. The data thus clearly show that there are two separate effects operating. One of the effects may dominate over the other in a given size domain. The relative strengths of these two effects will determine the size where the turnaround will occur. We propose the following explanation for the observed behavior.

The first effect that appears to come into play and may dominate in the early stage of size reduction ($d > 100$ nm) is the enhancement of T_C due to the enhancement of the bandwidth (W). We find that there is a likely enhancement of W on size reduction. An estimate of the bandwidth W (in the double exchange model) can be made from the relation [33, 34]

$$W \propto \cos\omega / d_{\mathrm{Mn-O}}^{3.5}, \tag{2}$$

where $\omega = \frac{1}{2}(\pi - \theta_{\mathrm{Mn-O-Mn}})$. Thus, an increase in the bond angle $\theta_{\mathrm{Mn-O-Mn}}$ and a decrease in the bond length $d_{\mathrm{Mn-O}}$ would mean an overall increase in the bandwidth W, thereby leading to an enhancement of T_C. As has been shown in figures 6 and 7, there are reductions of ω and $d_{\mathrm{Mn-O}}$ upon size reduction. Quantitatively, we can estimate the relative change in W using the values of $d_{\mathrm{Mn-O}}$ and $\theta_{\mathrm{Mn-O-Mn}}$ at T_C for a given size. For $d_{\mathrm{Mn-O}}$ and $\theta_{\mathrm{Mn-O-Mn}}$, we used the average of the two values for the two oxygen positions. For the smallest particle ($d = 15$ nm), the enhancement of W is more than 15% and the particle with $d = 50$ nm showing the largest enhancement in T_C (10%) has a relative enhancement in W of $\approx$6%. The enhancement of T_C can thus be linked to an enhancement of W upon size reduction. A simple phenomenological way of relating the shift in W (ΔW) with d will be to invoke the relation $\Delta W \propto d^{-n}$, where n is an exponent. One would thus expect that the change in T_C with size reduction arising from the bandwidth effects can be expressed phenomenologically as

$$\frac{T_C(d) - T_C(\infty)}{T_C(\infty)} = \left(\frac{d_0}{d}\right)^n, \tag{3}$$

where $T_C(\infty)$ and $T_C(d)$ are the values of T_C for the bulk sample and a particle of size d. d_0 is a length scale of nearly atomic dimensions.

The enhancement of T_C as d is reduced from the bulk (for $d > 50$ nm) observed in $La_{0.67}Ca_{0.33}MnO_3$ appears to be a special feature of the double-exchange ferromagnet that has a large sensitivity to the bandwidth. It is interesting to compare the size dependence of T_C in $La_{0.5}Sr_{0.5}CoO_3$, which is not a double-exchange ferromagnet. We investigated the ferromagnetic nanoparticles of $La_{0.5}Sr_{0.5}CoO_3$ in the size range $d = 35$–3000 nm synthesized using a similar chemical route. We found that in this system the behavior is qualitatively different and there is a monotonic depression of T_C with reduction in d. As the particle size was taken down to 35 nm there was a 20% reduction in T_C from the bulk value. This is unlike the scenario in manganites.

The second effect that will come into play and will tend to decrease the T_C is the finite-size effect that one would expect in magnetic systems of reduced dimensions such as in thin films, nanowires and nanoparticles [35]. This occurs when the size becomes comparable to the magnetic correlation length ξ, which cannot grow near the critical point due to finite size of the sample. For nanoparticles of elemental ferromagnetic materials this issue has been investigated, while for ferromagnetic oxide nanoparticles investigations of the size effects on T_C are limited [35]. In conventional elemental ferromagnetic nanowires and nanoparticles, this effect has been well established. The value of the correlation length at zero temperature ξ_0 sets the scale for the finite-size effect and for most conventional ferromagnetic systems

$\xi_0 \approx 2$–4 nm [36, 37]. Generally, the finite-size effect that leads to depression in T_C in magnetic systems is the relation [35]

$$\frac{T_C(\infty) - T_C(d)}{T_C(\infty)} = \left(\frac{\xi_0}{d}\right)^{\lambda}. \tag{4}$$

As an example of finite-size effects on the magnetic transitions in different nanomaterials, the value of $\lambda = 0.94$–0.98 with $\xi_0 = 2.2$–3.35 nm for Ni nanowires [36]. Finite-size effects have been investigated in oxide films [38] of $La_{0.7}Ca_{0.3}MnO_3$, where the values of λ and ξ_0 are 1.0 and 5 nm, respectively. For $La_{0.7}Sr_{0.3}CoO_3$ films the values are 0.8 and 2.3 nm, respectively.

For comparison we investigated the ferromagnetic nanoparticles of $La_{0.5}Sr_{0.5}CoO_3$ and observed the depression of T_C with d in the size range $d = 35$–3000 nm as stated before. From these data we find that $\lambda = 0.6$ and $\xi_0 = 3.4$ nm. This value of λ, although smaller than other systems, is very close to the theoretical predictions of $\lambda \approx 0.7$ [35].

The finite size effects need be separated from the effects that may arise from disordered surfaces, which will occur at layers of thickness δ. The finite size effects occur in the bulk or the core of the nanoparticle where the long-range spin order develops and gets truncated by the size of the particle. This needs to be distinguished from effects that arise from disordered spins at the surface. The surface layer with $M_S = 0$ has $T_C = 0$ and will not contribute to any magnetic transition. We did not observe any secondary transition below T_C which will rule out the effect of the surface layer on the determination of T_C. It acts only to limit the growth of ξ of the spins in the core so that the T_C is depressed by the finite size effect.

When the above two effects act in tandem, one trying to enhance the Curie temperature (due to enhancement of bandwidth upon size reduction) and the other to decrease it (due to finite size effect), one would see the non-monotonic behavior as seen by us. To quantitatively extract the parameters, we fit the data shown in figure 3 to the phenomenological relation

$$\frac{T_C(d) - T_C(\infty)}{T_C(\infty)} = \left(\frac{d_0}{d}\right)^{n} - \left(\frac{\xi_0}{d}\right)^{\lambda}. \tag{5}$$

The fit is shown in figure 3 along with the data. The exponents we obtain for the best fits are $n = 1.0$, $\lambda = 0.98$, $\xi_0 = 1.88$ nm and $d_0 = 1.71$ nm. The fit is reasonable and captures most of the data trend. The maximum deviation of the data from the fit $\delta T_C \approx 10$ K occurs near the peak for $d \approx 50$ nm. The exponents n and λ are close to 1, the microscopic spin correlation length ξ is very close to that seen in most ferromagentic materials. The microscopic length d_0 is of the order of 2 unit cells. The parameters obtained are all within reasonable physical limits. It thus appears that a combination of bandwidth-related enhancement and the finite size scaling can describe the dependence of T_C on d. The two effects being of similar magnitude, the variation of T_C with d may become very sensitive to factors such as preparation condition, etc which can change the balance.

4.3. Change in the nature of the phase transition

The change in the nature of the ferromagnetic-to-paramagnetic transition from first order to second order with size reduction is an interesting observation. As stated earlier, the order of the magnetic transition changes from first order to second order in size-reduced antiferromagnetic MnO. In the case of manganites, there are two issues to address that may be interrelated: one is the change in the nature of the transition and the other is the observation that the exponents are close to mean field value.

There can be a number of reasons that can change the nature of the transition. The presence of a size distribution can smear the transition region but will not change the nature of the transition. In fact, even in the bulk sample there is a size distribution that is comparable to that in the nanoparticles. But in the bulk sample, we see a very clear first-order transition. Thus, the smearing due to size distribution cannot be the cause of the change in the nature of the transition. This smearing will be like broadening due to temperature fluctuations [39].

The effect of quenched impurities on first-order transition has been studied theoretically [40] and experimentally [22], and it is argued that extensive disorder can transform a first-order transition into a second-order transition and the general criteria have been worked out. While a spread in local transition temperature arising from local disorder/impurity can cause the solid to break into a lower temperature phase and a higher temperature phase near the average transition to lower the bulk volume energy, this can be prevented by the energy cost of forming an interface between such phases that will stabilize the system against local phase fluctuations. In our case, there is no significant disorder or impurity that can cause a significant shift in the transition temperature. However, local strain fluctuations can cause fluctuations in the local T_C. From the XRD line shape the microstrain, which is the fluctuation in local strain, was found to be $\approx$0.8%. Using the bulk modulus ($\sim$150 GPa), the local pressure fluctuation can be worked out to be 1.2 GPa. In manganites, the transition temperature T_C has a pressure derivative value of $dT_C/dP \approx 20.2\,\mathrm{K\,GPa^{-1}}$. From this, we can estimate the order of the transition temperature changes arising from the static local strain fluctuations, which is $\delta T \approx 24$ K. This local fluctuation can smear out the transition by producing local phase fluctuations provided the interface energy needed is not large. The local transition temperature fluctuation that leads to local phase fluctuation occurs over a length scale l_0 determined by the interfacial energy, coherence length ξ_{coh} and the latent heat. If $\xi_{coh} > l_0$, the interface energy will stabilize the system against local fluctuations and there will be no significant smearing that can change the nature of the transition. On the other hand, when $\xi_{coh} < l_0$, the transition will be significantly smeared and the nature of the transition can change from first order to second order. However, given the fact that we are dealing with limited system sizes, for small samples ξ_{coh} can be limited by the system size d. In that case one may get a situation where l_0 can be comparable to d and one can get local phase fluctuations smearing out the transition. In the absence of such information as the interfacial energy, we cannot draw a definite conclusion on whether this local phase fluctuation can turn a first-order transition to a second-order transition although this a distinct possibility.

Another mechanism that is specific to the manganites and can lead to a change in the nature of the transition is the effect of bandwidth W. It has been established that in manganites when the bandwidth is increased without changing the carrier concentration (e.g. by substitution of ions with larger ionic radius in A site [24]), the nature of the transition can change from first order to second order. An estimate from the available structural data (for Sr- and Ca-substituted manganites) can be used to evaluate the change in bandwidth on substitution of Sr in place of Ca, using equation (2). The crossover occurs for rather low Sr substitution ($\sim$10%). This corresponds to a change in the bandwidth $W \sim 3$–5%. In our case, as discussed before, we do find that there is an enhancement in the bandwidth on size reduction which is of similar order. Thus, an enhancement of bandwidth that occurs upon size reduction can also change the order of the transition. In all probability, the random local strain fluctuations and the bandwidth enhancement act in tandem to change the nature of the transition.

The other issue is that the critical exponents measured from the magnetization data show values that are close to the mean field values. This would be expected in a system of finite size when the Ginzburg coherence length ξ_{coh} cannot grow beyond the system size so that order parameter fluctuations cannot grow so that the system stays close to the mean field region and the critical behavior is not observed [41]. An estimation of ξ_{coh} can be obtained from the bare microscopic coherence length and the heat capacity change ΔC_v at the transition [41]. From the depression of T_C with d (equation (5)), we obtain the microscopic coherence length $\approx$1.88 nm. Using experimentally determined values of C_V at the transition, we find that ξ_{coh} can grow as large as 1 μm. Since the particle size is much smaller, the system will stay close to the mean field region.

5. Conclusions

In summary, we have presented an extensive investigation of the effect of size reduction on the ferromagnetic state of LCMO using neutron diffraction along with magnetic measurements. The effects of finite size as seen on some of the physical properties has been analyzed. The analysis of the structural data shows a small but distinct compaction of the MnO_6 octahedron with smaller d_{Mn-O} and with $\theta_{Mn-O-Mn} \rightarrow 180^\circ$. This leads to an enhancement of the bandwidth. The neutron data show that even down to a size of 15 nm the nanoparticles retain ferromagnetic order as can be seen from reduced but finite spontaneous magnetization (M_S). The reduction in the spontaneous magnetization upon size reduction was explained as arising from a magnetic dead layer with $M_S \approx 0$ of thickness $\sim$2 nm. It is concluded that manganite nanoparticles with size below 5 nm may not have any M_S. The transition to ferromagnetic state changes over from a first-order transition to a second-order transition with critical exponents approaching mean field values. This was explained as arising from truncation of the coherence length by the finite sample size. The observed non-monotonic variation of the ferromagnetic transition T_C with size d was explained as arising from the simultaneous presence of two effects, one arising from bandwidth enhancement that makes the T_C larger, and the other a finite-size effect that reduces T_C. The latter effect wins over at smaller size and the crossover was found to occur in the size range around 50 nm.

Acknowledgments

We thank the Department of Science and Technology, Government of India for financial support in the form of a Unit for Nanoscience. TS thanks the UGC, Government of India for a fellowship.

References

[1] Dey P and Nath T K 2006 *Phys. Rev.* B **73** 214425
[2] Savosta M M, Krivoruchko V N, Danilenko I A, Tarenkov V, Konstantinova T E Yu, Borodin A V and Varyukhin V N 2004 *Phys. Rev.* B **69** 024413
[3] Zhang N, Ding W, Zhong W, Xing D and Du Y 1997 *Phys. Rev.* B **56** 8138
[4] Dutta A, Gayathri N and Ranganathan R 2003 *Phys. Rev.* B **68** 054432
[5] Rao S S, Tripathi S, Pandey D and Bhat S V 2006 *Phys. Rev.* B **74** 144416
[6] Biswas A and Das I 2006 *Phys. Rev.* B **74** 172405

[7] Zhu T, Shen B G, Sun J R, Zhao H W and Zhan W S 2001 *Appl. Phys. Lett.* **78** 3863
[8] Bibes M, Balcells Ll, Fontcuberta J, Wojcik M, Nadolski S and Jedryka E 2003 *Appl. Phys. Lett.* **82** 928
[9] Curiale J, Granada M, Troiani H E, Sanchez R D, Levya A G, Levy P and Samwer K 2009 *Appl. Phys. Lett.* **95** 043106
[10] Lopez-Quintela M A, Hueso L E, Rivas J and Rivadulla F 2003 *Nanotechnology* **14** 212
[11] Batlle X and Labarta A 2002 *J. Phys. D: Appl. Phys.* **35** R15
[12] Kodama R H 1999 *J. Magn. Magn. Mater.* **200** 359
[13] Rao C N R and Raveau B 1998 (ed) *Colossal Magnetoresistance, Charge Ordering and Related Properties of Manganese Oxides* (Singapore: World Scientific)
[14] Shantha K, Shankar Kar S, Subbanna G N and Raychaudhuri A K 2004 *Solid State Commun.* **129** 479
[15] Bhowmik R N, Poddar A, Ranganathan R and Majumdar C 2008 arXiv:0810.0090v1[cond-mat.mtrl-sci]
[16] Ziese M, Semmelhack H C, Han K H, Sena S P and Blythe H J 2002 *J. Appl. Phys.* **91** 9930
[17] Sarkar T, Ghosh B, Raychaudhuri A K and Chatterji T 2008 *Phys. Rev.* B **77** 235112
[18] Sarkar T, Raychaudhuri A K and Chatterji T 2008 *Appl. Phys. Lett.* **92** 123104
[19] Mira J, Rivas J, Rivadulla F, Vazquez-Vazquez C and Lopez-Quintela M A 1999 *Phys. Rev.* B **60** 2998
[20] Moutis N, Panagiotopoulos I, Pissas M and Niarchos D 1999 *Phys. Rev.* B **59** 1129
[21] Adams C P, Lynn J W, Smolyaninova V N, Biswas A, Greene R L, Ratcliff W II, Cheong S-W, Mukovskii Y M and Shulyatev D A 2004 *Phys. Rev.* B **70** 134414
[22] Roßler S, Roßler U K, Nenkov K, Eckert D, Yusuf S M, Dorr K and Muller K-H 2004 *Phys. Rev.* B **70** 104417
[23] Kim D, Revaz B, Zink B L, Hellman F, Rhyne J J and Mitchell J F 2002 *Phys. Rev. Lett.* **89** 227202
[24] Mira J, Rivas J, Rivadulla F and Lopez Quintela M A 2002 *Physica* B **320** 23
[25] Williamson G K and Hall W H 1953 *Acta Metall.* **1** 22
[26] http://www.ill.eu/sites/fullprof
[27] Martin M C, Shirane G, Endoh Y, Hirota K, Moritomo Y and Tokura Y 1996 *Phys. Rev.* B **53** 14285
[28] Banerjee B K 1964 *Phys. Lett.* **12** 16
[29] Golosovsky I V, Mirebeau I, Sakhnenko V P, Kurdyukov D A and Kumzerov Y A 2005 *Phys. Rev.* B **72** 144409
[30] Tang W, Lu W, Luo X, Wang B, Zhu X, Song W, Yang Z and Sun Y 2010 *J. Magn. Magn. Mater.* **322** 2360
[31] Kameli P, Salamati H and Aezami A 2006 *J. Appl. Phys.* **100** 053914
[32] Kar S, Sarkar J, Ghosh B and Raychaudhuri A K 2006 *Phys. Rev.* B **74** 085412
[33] Medarde M, Mesot J, Lacorre P, Rosenkranz S, Fischer P and Gobrecht K 1995 *Phys. Rev.* B **52** 9248
[34] Arulraj A, Santosh P N, Srinivasa Gopalan R, Guha A, Raychaudhuri A K, Kumar N and Rao C N R 1998 *J. Phys.: Condens. Matter* **10** 8497
[35] Barber M N 1983 *Phase Transitions and Critical Phenomena* ed C Domb and J L Lebowitz (New York: Academic)
[36] Sun L, Searson P C and Chien C L 2000 *Phys. Rev.* B **61** R6463
[37] Lutz H, Scoboria P, Crow J E and Mihalisin T 1978 *Phys. Rev.* B **18** 3600
[38] de Andres A, Rubio J, Castro G, Taboada S, Martinez J L and Colino J M 2003 *Appl. Phys. Lett.* **83** 713
[39] Imry Y 1980 *Phys. Rev.* B **21** 2042
[40] Imry Y and Wortis M 1979 *Phys. Rev.* B **19** 3580
[41] Chaikin P M and Lubensky T C 1995 *Principles of Condensed Matter Physics* (Cambridge: Cambridge University Press)